Desalination and Water Treatment
www.deswater.com
doi: 10.5004/dwt.2021.27173

224 (2021) 55–64
June

Comparative study of a conventional solar still with different basin materials using exergy analysis

Mohammed El Hadi Attia[a], A. Muthu Manokar[b], Abd Elnaby Kabeel[c,d], Zied Driss[e], Ravishankar Sathyamurthy[f], Wael Al-Kouz[g,*]

[a]*Department of Physics, Faculty of Science, University of El Oued, 39000 El Oued, Algeria, email: attiameh@gmail.com*
[b]*Department of Mechanical Engineering, B.S. Abdur Rahman Crescent Institute of Science and Technology, Chennai-600 048, Tamil Nadu, India, email: a.muthumanokar@gmail.com*
[c]*Mechanical Power Engineering Department, Faculty of Engineering, Tanta University, Tanta, Egypt, email: kabeel6@f-eng.tanta.edu.eg*
[d]*Faculty of Engineering, Delta University for Science and Technology, Gamasa, Egypt, email: kabeel6@hotmail.com*
[e]*Laboratory of Electromechanical Systems, National School of Engineers of Sfax, University of Sfax, BP 1173, 3038, Sfax, Tunisia, email: zied.driss@enis.tn*
[f]*Department of Mechanical Engineering, KPR Institute of Engineering and Technology, Arasur, Coimbatore-641407, Tamil Nadu, India, email: raviannauniv23@gmail.com*
[g]*Mechanical Engineering Department, Prince Mohammad Bin Fahd University, Al Khobar, Kingdom of Saudi Arabia, email: walkouz@pmu.edu.sa*

Received 1 October 2020; Accepted 24 February 2021

A B S T R A C T

Among today's world problems, drinking water shortage is one important thing. Solar distillation is a simple and efficient solution to solve this problem, but the yield produced from solar distillation is low. The incorporation of thermal energy storage materials in the solar still is one of the solutions to enhance the yield. For enhancing the yield, solar stills were fabricated using high thermal conductivity materials and tested on three consecutive days in June 2020 in the same climatic conditions. Three solar stills are single slope solar still with a steel plate (SSS-SP), SSS with a zinc plate (SSS-ZP) and SSS with a copper plate (SSS-CP). The maximum total drinkable water production from the SSS-SP, SSS-ZP and SSS-CP is equal to 3.35, 3.96 and 4.51 kg/m^2, respectively. The daily drinkable water production increased by 18.21% when using zinc plates and 34.63% when using the copper plate, related to the SSS-SP. The maximum daily exergy efficiency of the SSS-SP, SSS-ZP and SSS-CP are equal to 1.9%, 2.39% and 3.08%, respectively. The daily exergy efficiency was increased by 26.13% when using zinc plate and by 61.57% when using the copper plate, compared to the SSS-SP.

Keywords: Solar energy; Zinc plate; Copper plate; Energy storage; Freshwater

1. Introduction

Desalination using solar energy is an efficient solution for bringing distilled water, especially in remote areas that lack safe water due to the infrastructure and the no connection to the main national water network [1–3]. On the other hand, a solar distillation system can be a practical and economical way to produce distilled water, because remote areas possess large stocks of saltwater and abundant solar radiation [4]. The traditional solar distillery is one of the simplest types. Research has started direction towards improving techniques for producing freshwater from briny

* Corresponding author.

water by solar energy, and development of new types of solar distillers and the invention of other materials suitable to be good thermal storage materials [5–7]. Okeke et al. [8] used different sizes of charcoal (fine particles and pieces) in a single slope solar still (SSS). The researchers concluded that charcoal improves SSS performance. Rajvanshi [9] investigated the implementation of various dyes as absorbers materials in the SSS. The outcome confirmed that black naphthylamine dye can be enhanced the performance of the SSS. Sodha et al. [10] did the experiments using dyes (red, violet and black color) in a SSS. Experimental outcome reported that uses of violet and black dyes are suitable as compared to red dye. Akash et al. [11] reported the effect of different absorbing materials: black dyes, black ink and black rubber mat on the thermal performance of the SSS. The researchers found that black dyes had a better rate of production compared to other materials. El-Sebaii et al. [12] tested the effect of different absorbing plates: mica, aluminum, copper and stainless steel on the SSS performance. The researchers found that mica plates had a better production rate than aluminum, copper, and stainless steel plates. Nafey et al. [13] conducted experimental studies of different sizes of black rubber with a thickness of 10 mm and black gravel with a size of 20–30 mm thick in SSS. The results confirmed that black rubber and black gravel improves SSS performance. Murugavel et al. [14] reported the effect of aluminum rectangular fins enclosed with cotton and jute cloth on the performance of the solar distillate. Srivastava and Agrawal [15] researched SSS with porous absorbers and found that productivity was improved by 68% on a clear day, and it was improved by 35% on cloudy days. Shanmugan [16] considered different absorbing materials such as concrete stones, pebbles, and black granite stones on SSS performance. It was found that the SSS with concrete stones gave higher performance compared to other energy storage materials. Shanmuga Priya and Mahadi [17] performed an experimental investigation using black dye at concentrations equal to 20, 30, 50 and 70 ppm. It was concluded that evaporation rates improve when the black dye concentration is from 20 to 50 ppm. Indeed, when the concentration is changed from 50 to 70 ppm, the evaporation rate remains the same. Arjunan et al. [18] published a comparative study of SSS with and without energy storage materials (black granite gravels, pebbles, blue metal stones and paraffin wax). The researchers concluded that the use of black granite gravels was best as compared to others. In addition, its efficiency is 10.06% higher than the SSS. Dumka et al. [19] studied the impact of sand-filled cotton bags on the productivity of SSS. The outcome confirmed that the distillate production was about 3,493 mL/d.m^2 with sand-filled cotton bags and about 2,717 mL/d.m^2 without sand-filled cotton bags. The solar still was fabricated using different materials such as plastic [20–25], fiber-reinforced plastic (FRP) [26–36], glass [37–44], acrylic [45–49] copper [50–56], concrete materials [57–59], and solar panel [60–67].

The aim of this experimental study is to improve the output of solar distillation by placing black painted copper and zinc plates. The presence of metal plates at the bottom of the basin enhanced the heat storage capacity. Thus a comparison of three solar distiller's performance has been carried out. The first distiller is considered as a reference, the second is the modified solar basin with the zinc metal plate, and the third is the modified solar basin with the copper metal plate. These experiments were conducted in the city of El Oued, Algeria, on three consecutive days in June 2020.

2. Experimental setup

Algeria has a huge amount of solar energy because of its unique location (Fig. 1). The mean duration of sunlight in the Algerian lands exceeds 2,000 h/y, to reach nearly 3,500 h/y in the desert. The total energy received is 169,400 TWh/y and it is 5,000 times the country's yearly power utilization.

The schematic and experimental set-up is shown in Figs. 2 and 3, respectively. This system presents a square base with an edge equal to 50 cm. The glass cover (3 mm thick) is tilted at an angle of 10°. The basin is made of wood with a thickness of 2.5 cm, and it is painted with black silicon, the front sidewall height is 6 cm, and the other side height is 14 cm. In addition, a PVC tube is attached to collect condensed water that flows over the glass surface. The testing was supervised for 3 d for the period of 6 to 8th June 2020 for 11 h in the city of El Oued Algeria located at 06° 47′ E and 33° 30′ N. On the bottom of the basins, black painted metal plates of zinc and copper were placed. These plates present a square base with an edge of 49.5 cm and a width of 0.2 cm. The metal plates have good physical and chemical properties that make them excellent energy storage materials. Table 1 shows the properties of the basin materials. Table 2 shows the error values committed in the measuring devices.

3. Results and discussions

3.1. Time-wise variation of solar intensity [I(t)], atmosphere (T_a), salty water ($T_{s.w}$), and collector cover ($T_{c.c}$) temperatures

Figs. 4–6 display the time-wise variation of $I(t)$, T_a, $T_{s.w}$, $T_{c.c}$ and SSS with a steel plate (SSS-SP), SSS with a zinc plate (SSS-ZP) and SSS with a copper plate (SSS-CP) on 6-6-2020 and 8-6-2020, respectively. From graph 4, it is known that $I(t)$ increases in the sunrise period and measured its highest value of 1,008 W/m^2 at 12 P.M. on 6-6-2020 and 995 W/m^2 at 12 P.M. on 8-6-2020. Also, T_a increased in the sunrise period and measured its highest value of 42°C at 1 P.M. on 6-6-2020 and 41°C at 1 P.M. on 8-6-2020. Time-wise variations of T_a, $T_{s.w}$ and $T_{c.c}$ have similar trends like $I(t)$ because it is the cause for variations of T_a, $T_{s.w}$ and $T_{c.c}$. The everyday mean value of $I(t)$ and T_a on 6-6-2020 are 673.17 W/m^2, and 36.83°C, respectively and on 8-6-2020 is 659.58 W/m^2, and 35.58°C, respectively. From Table 3, it is found that maximum $T_{s.w}$ of the SSS-ZP and SSS-CP is 2°C and 4°C higher than the SSS-SP on 6-6-2020 and maximum $T_{s.w}$ of the SSS-ZP and SSS-CP is 2°C and 3°C higher than the SSS-SP on 8-6-2020. The average daily $T_{s.w}$ of the SSS-ZP and SSS-CP is 3.52% and 6.88% higher than the SSS-SP on 6-6-2020, and the average daily $T_{s.w}$ of the SSS-ZP and SSS-CP is 2.51% and 6.08% higher than the SSS-SP on 8-6-2020. The average daily $T_{s.w}$ of the SSS-CP is 3.25% higher than the SSS-ZP on 6-6-2020, and the average daily $T_{s.w}$ of the SSS-CP is 3.49% higher than the SSS-ZP on 8-6-2020. Due to higher thermal conductivity materials in the SSS-CP and

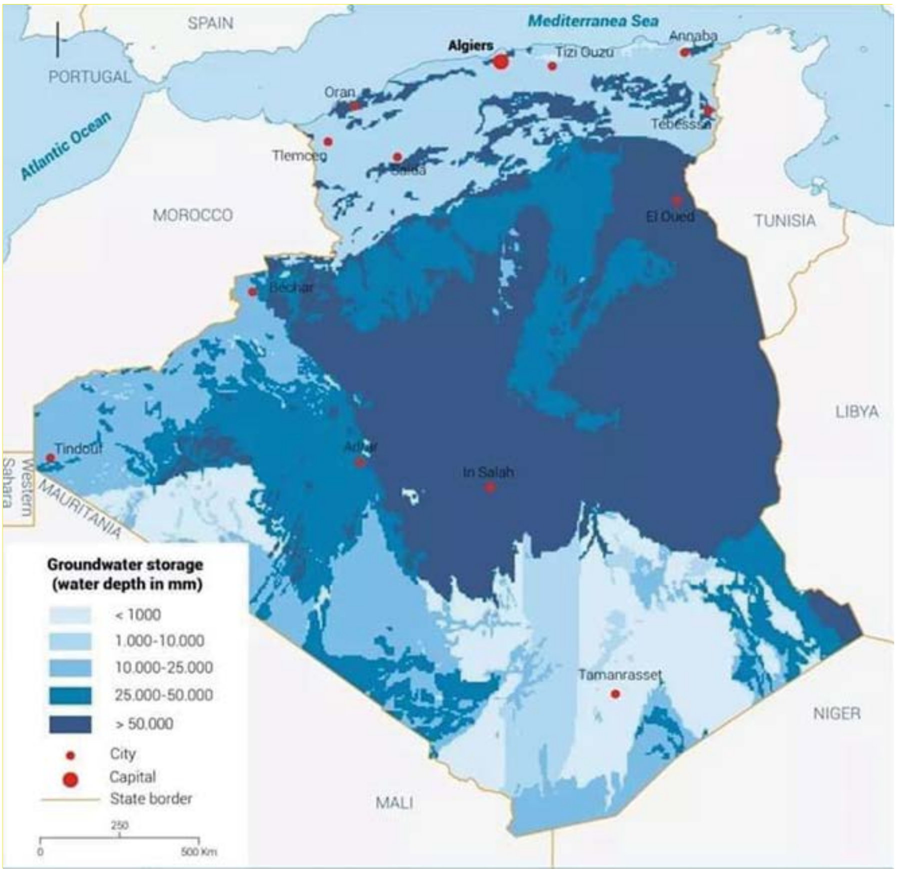

Fig. 1. Map of Algeria and the location of the groundwater [68].

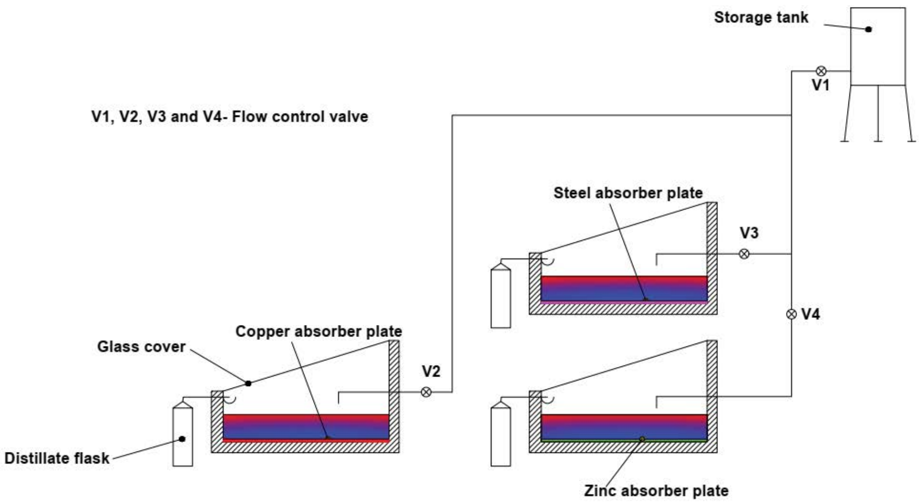

Fig. 2. Schematic of the solar distillers.

SSS-ZP, the maximum and daily average $T_{s.w}$ is higher than the SSS-SP. From Fig. 6, the highest $T_{c.c}$ of 53, 54 and 55°C was recorded on 6-6-2020 and 49°C, 51°C and 51°C was recorded on 8-6-2020 for the SSS-SP, SSS-ZP and SSS-CP, correspondingly. The daily mean $T_{c.c}$ of the SSS-SP, SSS-ZP and SSS-CP are 42°C, 42.75°C and 43.83°C on 6-6-2020 and 40.67°C, 40.98°C and 41.17°C on 8-6-2020. The zinc plate and copper plate used in the SSS-ZP and SSS-CP were used to improve the $T_{s.w}$ during evening time. So the incorporation of zinc plate and copper plate materials stores heat energy, and it improves the $T_{s.w}$ by adding heat energy to the saline water.

Fig. 3. Solar distillers.

Table 1
Properties of basin materials (steel, copper and zinc) [69,70]

Properties	Steel	Copper	Zinc
Density (kg/m^3)	7,870	8,960	7,133
Specific heat capacity (J/kg K)	456	385	390
Thermal conductivity W/(m K)	75	401	112

Table 2
Standard uncertainties

Instrument	Accuracy	Range	Standard uncertainty
Solar power meter (W/m^2)	±10	0–1,999	5.72
Thermocouple (°C)	±0.1	−100–500	0.07
Measuring jar (mL)	±1	0–250	0.6 mL

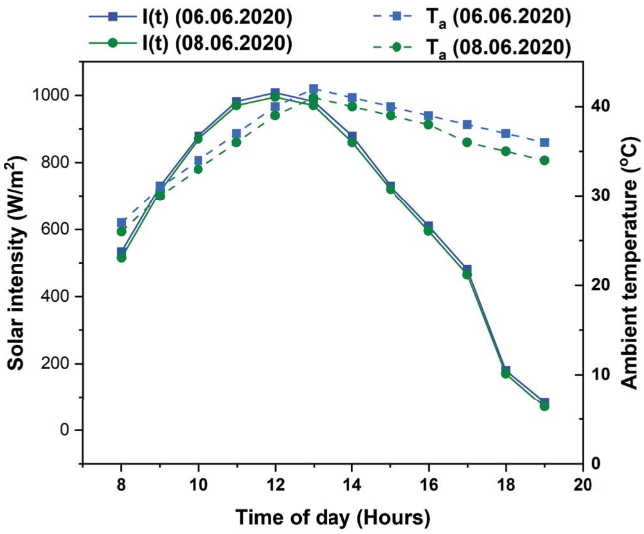

Fig. 4. Time-wise variation of $I(t)$ and T_a for on 6-6-2020 and 8-6-2020.

3.2. *Time-wise variation of evaporative heat transfer coefficient and hourly potable water production*

Figs. 7 and 8 display the time-wise difference of evaporative heat transfer coefficient (EHTC) and hourly production of potable water from the SSS-SP, SSS-ZP and SSS-CP on 6-6-2020 and 8-6-2020, respectively. Table 4 summarizes the maximum and average EHTC of the SSS-SP, SSS-ZP and SSS-CP on 6-6-2020 and 8-6-2020. The daily mean EHTC of the SSS-CP is higher than the SSS-SP, SSS-ZP due to the higher thermal conductivity copper plate. The daily average EHTC value of the SSS-ZP and SSS-CP is 9.41% and 19.21% higher than the average daily EHTC of the SSS-SP, and the daily average EHTC value of the SSS-CP is 8.96% higher as compared to the SSS-ZP. In the SSS-CP, the copper plate enhances the water temperature, and so it has higher hourly and average daily EHTC than the SSS-ZP and SSS-SP.

Figs. 7 and 8 show the potable water produced from a modified absorber on two different conditions. It is found that potable water production from the SSS-SP, SSS-ZP, and SSS-CP is increasing during the sunrise period and decreases during sunset periods. The highest potable water of 0.67, 0.77 and 0.88 kg was produced on 6-6-2020 and 0.63, 0.75 and 0.86 kg on 8-6-2020 from the SSS-SP, SSS-ZP and SSS-CP, respectively. The daily potable water production from the SSS-SP on 6-6-2020 is 3.35 kg and on 8-6-2020 is 3.19 kg, from the SSS-ZP on 6-6-2020 is 3.96 kg and on 8-6-2020 is 3.84 kg, from the SSS-CP on 6-6-2020 is 4.51 kg and on 8-6-2020 is 4.37 kg. When using the copper plate in the SSS, potable water production was augmented by about 18.3% and 34.59% on 6-6-2020 and 20.26% and 36.87% on 8-6-2020 as compared to SSS-ZP, SSS-SP, respectively. In the SSS-CP, due to the material properties, it stores the heat energy in the plate surface, and it reduces the heat losses from the SSS basin to the atmosphere so potable water production from the SSS-CP is higher as compared to the SSS-SP and SSS-ZP.

3.3. *Time-wise variation of energy and exergy efficiencies*

Time-wise difference of energy and exergy efficiencies of the SSS-SP, SSS-ZP and SSS-CP on 6-6-2020 and

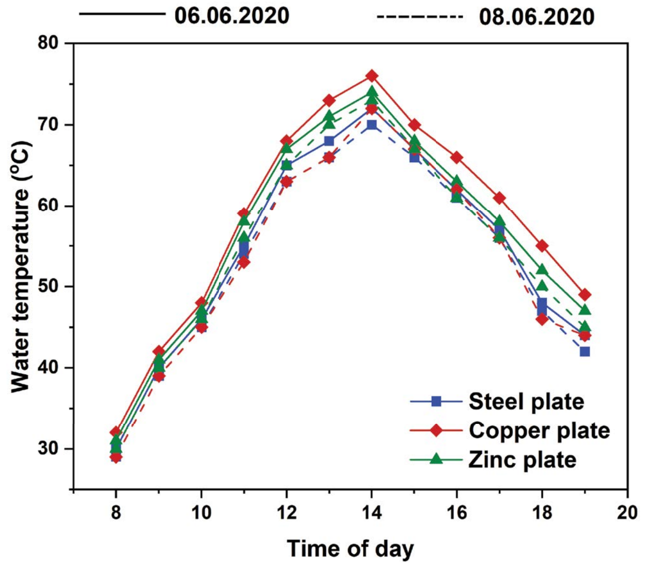

Fig. 5. Time-wise variation of $T_{s.w}$ for the SSS-SP, SSS-ZP and SSS-CP on 6-6-2020 and 8-6-2020.

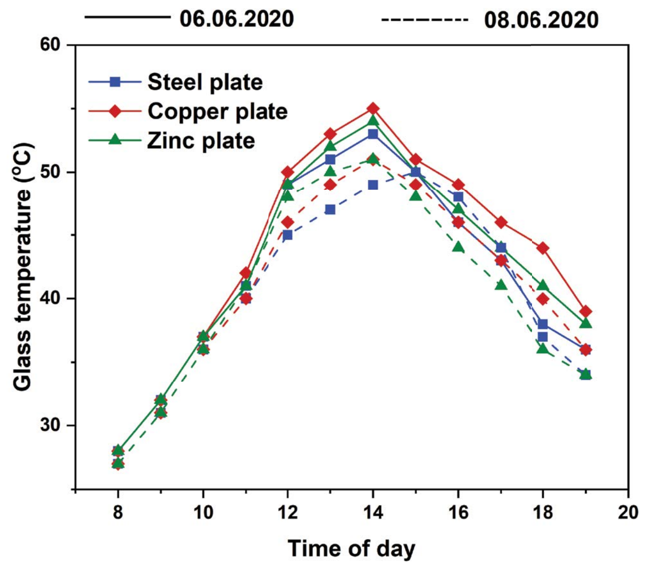

Fig. 6. Time-wise variation of $T_{c.c}$ for the SSS-SP, SSS-ZP and SSS-CP on 6-6-2020 and 8-6-2020.

Table 3
Maximum and average $T_{s.w}$ of the SSS-SP, SSS-ZP and SSS-CP

S. No	Date	Parameter	SSS-SP	SSS-ZP	SSS-CP
1	6-6-2020	Maximum $T_{s.w}$ (°C)	72	74	76
2	6-6-2020	Average $T_{s.w}$ (°C)	54.5	56.42	58.25
3	8-6-2020	Maximum $T_{s.w}$ (°C)	70	72	73
4	8-6-2020	Average $T_{s.w}$ (°C)	53.17	54.5	56.4

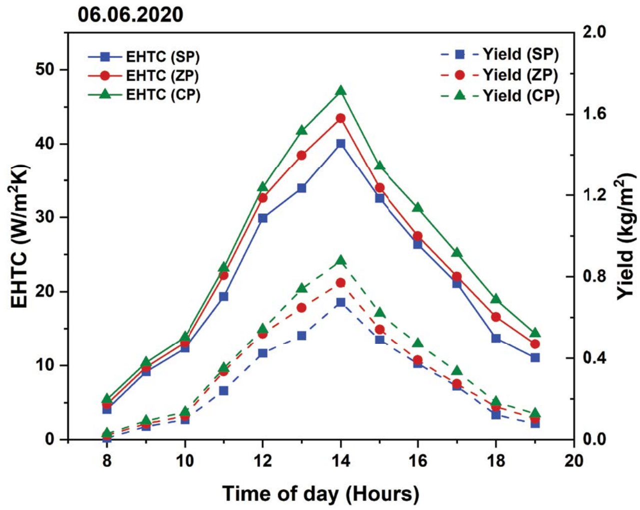

Fig. 7. Time-wise variation of EHTC and hourly potable water production from the SSS-SP, SSS-ZP and SSS-CP on 6-6-2020.

8-6-2020 are shown in Figs. 9 and 10. The SSS-SP, SSS-ZP and SSS-CP energy efficiency is increasing during the sunrise period and reached a maximum value at 2 P.M., and then it decreases up to 5 P.M., and again it starts increasing. The energy efficiency of the SSS-SP starts with 0.85% at 8 A.M., having an increasing trend and reached 48.12% at 2 P.M. and then it has a decreasing trend up to 5 P.M. (34.21%) and after 5 P.M. it was increasing and reached maximum efficiency of 49.79% at 7 P.M. Also energy efficiency of the SSS-ZP starts at 1.5% at 8 A.M., having an increasing trend and reached 51.95% at 2 P.M. and then it has a decreasing trend up to 5 P.M (35.72%) and after 5 P.M it is increasing and reached maximum efficiency of 56.63% at 7 P.M. Similarly, the energy efficiency of the SSS-CP starts at 2.26% at 8 A.M., having to increase trend and reached 61.53% at 2 P.M. and then it has a decreasing trend up to 5 P.M. (36.70%) and after 5 P.M. it was increasing and reached the maximum efficiency of 65.74% at 7 P.M. Table 5 summarizes the daily average energy and exergy efficiency of the SSS-SP, SSS-ZP and SSS-CP on 6-6-2020 and 8-6-2020. The energy efficiency of the SSS-CP is 24.4 and 14.14% higher than SSS-SP and SSS-ZP on 6-6-2020 and 25.56 and 14.3% higher than SSS-SP and SSS-ZP on 8-6-2020, respectively. The copper plate presence in the SSS-CP enhances the water temperature, EHTC and potable water production. Hence, it produced higher energy efficiency than the SSS-ZP and SSS-CP.

The exergy efficiency of the SSS-SP, SSS-ZP and SSS-CP is increasing during the sunrise period and reached a maximum value at 2 P.M., and then it decreases up to 6 P.M., and again it starts increasing. The exergy efficiency of the SSS-SP starts at 0.01% at 8 A.M., having an increasing trend and reached 4.65% at 2 P.M. and then it is decreasing trend up to 6 P.M. (1.56%) and after 6 P.M. it was increased and reached exergy efficiency of 1.97% on 7 P.M. Also exergy efficiency of the SSS-ZP starts with 0.04% at 8 A.M., having an increasing trend and reached 5.62% at 2 P.M. and then it has

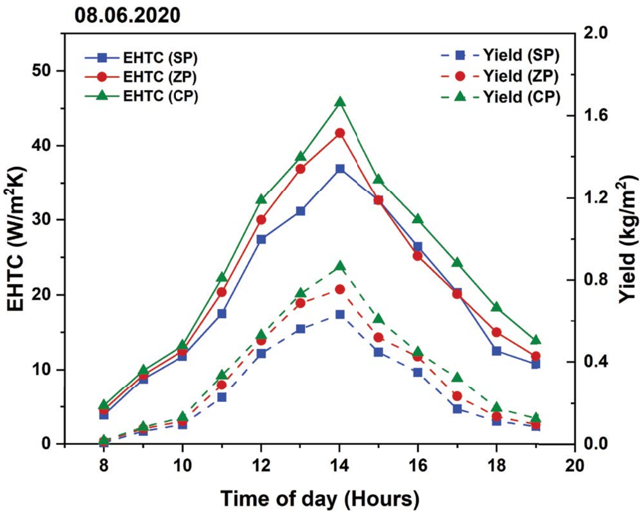

Fig. 8. Time-wise variation of EHTC and hourly potable water production from the SSS-SP, SSS-ZP and SSS-CP on 8-6-2020.

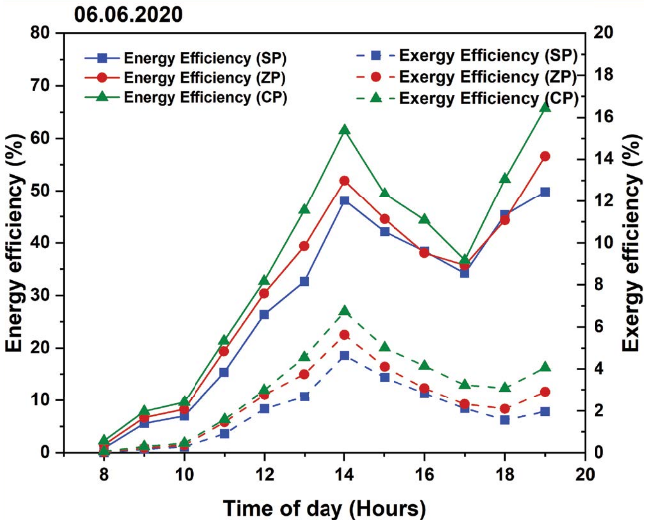

Fig. 9. Time-wise difference of energy and exergy efficiency of the SSS-SP, SSS-ZP and SSS-CP on 6-6-2020.

Table 4
Maximum and average EHTC of the SSS-SP, SSS-ZP and SSS-CP

S. No	Date	Parameter	SSS-SP	SSS-ZP	SSS-CP
1	6-6-2020	Maximum EHTC (W/m^2 K)	40.07	43.47	47.11
2	6-6-2020	Average EHTC (W/m^2 K)	21.13	23.12	25.19
3	8-6-2020	Maximum EHTC (W/m^2 K)	36.93	41.69	45.75
4	8-6-2020	Average EHTC (W/m^2 K)	20	21.67	24.1

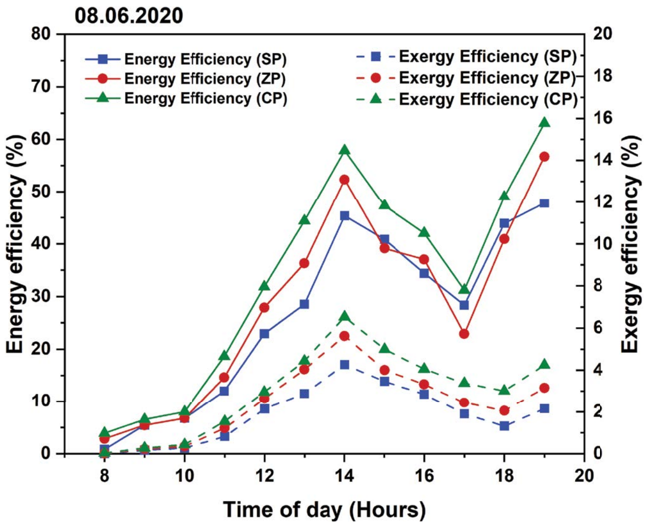

Fig. 10. Time-wise difference of energy and exergy efficiency of the SSS-SP, SSS-ZP and SSS-CP on 8-6-2020.

a decreasing trend up to 6 P.M. (2.09%) and after 6 P.M. it was increasing and reached an efficiency of 2.9% at 7 P.M. Similarly the exergy efficiency of the SSS-CP starts with 0.06% at 8 A.M., having an increasing trend and reached 6.74% at 2 P.M. and then it has a decreasing trend up to 6 P.M. (3.09%) and after 6 P.M. it was increasing and reached an efficiency of 4.06% at 7 P.M. The exergy efficiency of the SSS-CP is 58.43% and 26.13% higher than SSS-SP and SSS-ZP on 6-6-2020 and 61.57% and 23.42% higher than SSS-SP and SSS-ZP on 8-6-2020, respectively. The solar still exergy efficiency is maximum in the case of the copper plate because exergy efficiency is directly related to potable water production and available solar intensity. During the evening time, the difference between $T_{s.w}$ and $T_{c.c}$ is higher, so it is higher at the time of the evening compared to the morning.

3.4. Comparison of similar studies

In Table 6, the comparison of present results with the daily productivity of other published works has been summarized. From the results, it has been noted that the daily yield of a SSS containing zinc metal plate increases by 18.21% compared to the SSS-SP and cumulative yield increases by 34.63% when using the copper metal plate. Thus, the copper metal plate greatly enhances the productivity of solar distillation. From Table 6 it can be summarized the productivity of plastic solar still (Cappelletti [20]) is minimum (1.8 $kg/m^2/d$) and copper solar still (Abujazar et al. [50]) is (4.383 $kg/m^2/d$), and solar panel solar still is (7.3 kg). The present study produced maximum productivity of 3.96 and 4.51 kg using zinc steel plate and copper steel plate, respectively.

4. Economic evaluation

Table 7 shows the fabrication cost of the SSS-SP, SSS-ZP and SSS-CP. From these results, it is clear that the maximum value of the amount of water produced during the day is obtained with the SSS-CP and it is equal to

Table 5
Maximum and average $T_{s.w}$ of the SSS-SP, SSS-ZP and SSS-CP

S. No	Date	Parameter	SSS-SP	SSS-ZP	SSS-CP
1	6-6-2020	Average energy efficiency (%)	28.81	31.40	35.84
2	8-6-2020	Average energy efficiency (%)	26.43	29.03	33.19
3	6-6-2020	Average exergy efficiency (%)	1.9	2.39	3.02
4	8-6-2020	Average exergy efficiency (%)	1.85	2.42	2.99

Table 6
Comparison between the accumulated productivity of previously published works and our experimental work

Authors and reference	Types of solar still	Yield (kg/m^2/d)
Cappelletti [20]	Plastic solar still	1.8
Tiwari and Mohamed Selim [26]	FRP solar still	4.5
Rajaseenivasan et al. [38]	Glass solar still	3.61
Manokar and Winston [45]	Acrylic solar still	2.64
Abujazar et al. [50]	Copper solar still	4.383
Manokar et al. [60]	Solar panel integrated solar still	7.3
Present experimental work	CSS	3.35
	With zinc metal plate	3.96
	With copper metal plate	4.51

Table 7
Fabrication cost of the SSS-SP, SSS-ZP and SSS-CP (1$ = 112.78 DZD; 1€ = 136.03 DZD)

	SSS-SP (steel plate)	SSS-ZP (zinc metal plate)	SSS-CP (copper metal plate)
Total cost of manufacture (DZD)	2,000	2,000	2,000
Price of metal plate	–	37.5	150
Maintenance cost (DZD)	12.5	12.5	12.5
Total cost (DZD)	2,012.5	2,050	2,162.5
Daily yield collected (kg/0.25 m^2/d)	0.84	0.99	1.12
Cost per liter of distilled water on the market (DZD)	60	60	60
Price of daily water production (DZD)	50.25	59.4	67.65
Recovery period (d)	40	35	32

4.51 kg/m^2/d with a price of daily water production equal to 270.6 DZD. The cost recovery period for the SSS-SP, SSS-ZP and SSS-CP is 40, 35 and 32 d, respectively.

5. Conclusions

Modification of the solar still was made by the addition of metal plates of steel, zinc and copper. A comparison was made between steel, zinc and copper plates. The following conclusions are obtained:

- Copper and zinc metal plates enhance the efficiency of solar stills due to its high thermal conductivity.
- Using the copper metal plate as thermal storage material is much better than using zinc metal plates.
- By using the SSS-SP, the production of the distilled water is equal to 3.35 kg/m^2.
- By using the SSS-ZP, the production of the distilled water is equal to 3.96 kg/m^2.
- By using the SSS-CP, the production of the distilled water is equal to 4.51 kg/m^2.
- SSS-CP productivity increases to about a higher rate of 14% as compared to SSS-ZP.
- Compared to the SSS-SP, the daily accumulation was improved by 18.21% and 34.63% by using a metal plate zinc and copper, respectively.

The solar still with zinc and copper plates augment the output of the distillation and increase efficiency. Therefore, copper metal plates are excellent energy storage materials and are recommended in such applications.

References

[1] M. El Hadi Attia, Z. Driss, A.E. Kabeel, M. Abdelgaied, A.M. Manokar, R. Sathyamurthy, A.K. Hussein, Performance evaluation of modified solar still using aluminum foil sheet as absorber cover – a comparative study, J. Test. Eval., 49 (2021), doi: 10.1520/JTE20200249.

[2] A. Khechekhouche, A.E. Kabeel, B. Benhaoua, M. El Hadi Attia, E.M.S. El-said, Traditional solar distiller improvement by a single external refractor under the climatic conditions of the El-Oued region, Algeria, Desal. Water Treat., 177 (2020) 23–28.
[3] A.E. Kabeel, M. Abdelgaied, A. Eisa, Enhancing the performance of single basin solar still using high thermal conductivity sensible storage materials, J. Cleaner Prod., 183 (2018) 20–25.
[4] A. Khechekhouche, B. Benhaoua, M. El Hadi Attia, Z. Driss, A. Manokar, M. Ghodbane, Polluted groundwater treatment in southeastern Algeria by solar distillation, Algerian J. Environ. Sci. Technol., 6 (2020) 1207–1211.
[5] S. Vaithilingam, S.T. Gopal, S.K. Srinivasan, A. Muthu Manokar, R. Sathyamurthy, G.S. Esakkimuthu, R. Kumar, M. Sharifpur, An extensive review on thermodynamic aspect based solar desalination techniques, J. Therm. Anal. Calorim., (2020), doi: 10.1007/s10973-020-10269-x.
[6] A. Khechekhouche, B.B. Haoua, A.E. Kabeel, M. El Hadi Attia, W.M. El-Maghlany, Improvement of solar distiller productivity by a black metallic plate of zinc as a thermal storage material, J. Test. Eval., 49 (2021) 967–976.
[7] M. El Hadi Attia, Z. Driss, A.M. Manokar, R. Sathyamurthy, Effect of aluminum balls on the productivity of solar distillate, J. Storage Mater., 30 (2020) 101466, doi: 10.1016/j.est.2020.101466.
[8] C.E. Okeke, S.U. Egarievwe, A.O.E. Animalu, Effects of coal and charcoal on solar-still performance, Energy, 15 (1990) 1071–1073.
[9] A.K. Rajvanshi, Effect of various dyes on solar distillation, Sol. Energy, 27 (1981) 51–65.
[10] M.S. Sodha, A. Kumar, G.N. Tiwari, G.C. Pandey, Effects of dye on the performance of a solar still, Appl. Energy, 7 (1980) 147–162.
[11] B.A. Akash, M.S. Mohsen, O. Osta, Y. Elayan, Experimental evaluation of a single-basin solar still using different absorbing materials, Renewable Energy, 14 (1998) 307–310.
[12] A.A. El-Sebaii, S. Aboul-Enein, M.R.I. Ramadan, E. El-Bialy, Year-round performance of a modified single-basin solar still with mica plate as a suspended absorber, Energy, 25 (2000) 35–49.
[13] A.S. Nafey, M. Abdelkader, A. Abdelmotalip, A.A. Mabrouk, Solar still productivity enhancement, Energy Convers. Manage., 42 (2001) 1401–1408.
[14] K.K. Murugavel, K. Srithar, Performance study on basin type double slope solar still with different wick materials and minimum mass of water, Renewable Energy, 36 (2011) 612–620.
[15] P.K. Srivastava, S.K. Agrawal, Experimental and theoretical analysis of single sloped basin type solar still consisting of multiple low thermal inertia floating porous absorbers, Desalination, 311 (2013) 198–205.
[16] Dr. S. Shanmugan, Experimental investigation of various energy absorbing materials on performance of single slope single basin solar still with hot water provision, Int. J. Innovative Res. Sci. Eng. Technol., 2 (2013) 7760–7767.
[17] S. Shanmuga Priya, U.I. Mahadi, Effect of different absorbing materials on solar distillation under the climatic condition of Manipal, Int. J. Appl. Innovation Eng. Manage., 2 (2013) 301–304.
[18] T.V. Arjunan, H.S. Aybar, P. Sadagopan, B.S. Chandran, S. Neelakrishnan, N. Nedunchezhian, The effect of energy storage materials on the performance of a simple solar still, Energy Sources Part A, 36 (2014) 131–141.
[19] P. Dumka, A. Sharma, Y. Kushwah, A.S. Raghav, D.R. Mishra, Performance evaluation of single slope solar still augmented with sand-filled cotton bags, J. Storage Mater., 25 (2019) 100888, doi: 10.1016/j.est.2019.100888.
[20] G.M. Cappelletti, An experiment with a plastic solar still, Desalination, 142 (2002) 221–227.
[21] M.K. Phadatare, S.K. Verma, Influence of water depth on internal heat and mass transfer in a plastic solar still, Desalination, 217 (2007) 267–275.
[22] R. Bhardwaj, M.V. ten Kortenaar, R.F. Mudde, Inflatable plastic solar still with passive condenser for single family use, Desalination, 398 (2016) 151–156.
[23] S.H. Sengar, Y.P. Khandetod, A.G. Mohod, New Innovation of low cost solar still, Eur. Int. J. Sustainable Dev., 1 (2012) 315–315.
[24] J.A. Duffie, New materials in solar energy utilization, Sol. Energy, 6 (1962) 114–118.
[25] D. Mugisidi, O. Heriyani, H. Fathurahman, Comparison of plastic and stainless-steel as solar still material, IOP Conf. Ser.: Mater. Sci. Eng., 403 (2018) 012089.
[26] G.N. Tiwari, G.A. Mohamed Selim, Double slope fibre reinforced plastic (FRP) multiwick solar still, Solar Wind Technol., 1 (1984) 229–235.
[27] Y.P. Yadav, G.N. Tiwari, Monthly comparative performance of solar stills of various designs, Desalination, 67 (1987) 565–578.
[28] Y.P. Yadav, G.N. Tiwari, Demonstration plants of fibre reinforced plastic multiwick solar still: an experimental study, Solar Wind Technol., 6 (1989) 653–666.
[29] G.N. Tiwari, A.K. Singh, Thermal efficiency of double slope FRP solar distiller: an analytical and experimental studies, Desalination, 82 (1991) 221.
[30] A.Kr. Tiwari, A. Somwanshi, Techno-economic analysis of mini solar distillation plants integrated with reservoir of garden fountain for hot and dry climate of Jodhpur (India), Sol. Energy, 160 (2018) 216–224.
[31] P. Pal, R. Dev, Experimental study on modified double slope solar still and modified basin type double slope multiwick solar still, Int. J. Civ. Environ. Eng., 10 (2016) 70–75.
[32] S. Kumar, G.N. Tiwari, Performance evaluation of an active solar distillation system, Energy, 21 (1996) 805–808.
[33] V. Ramanathan, B. Kanimozhi, V.K. Bhojwani, Experimental study on productivity of modified single-basin solar still with a flat plate absorber, IOP Conf. Ser.: Mater. Sci. Eng., 197 (2017) 012032.
[34] G.N. Tiwari, Feasibility study of solar distillation plants in south pacific countries, Desalination, 83 (1991) 223–232.
[35] V. Krishnaswamy, R. Ali, M. Vedpathak, Experimental Investigation of V-Type Solar Still Coupled with Solar Water Heater, SSRN Electronic Journal, Mahatma Education Society's Transactions and Journals' Conference Proceedings, Conference on Technologies for Future Cities (CTFC), 2019, pp. 1–6. Available at: http://ssrn.com/link/2019-CTFC.html
[36] P. Pal, A.K. Nayak, R. Dev, A modified double slope basin type solar distiller: experimental and enviro–economic study, EVERGREEN Joint J. Novel Carbon Resour. Sci. Green Asia Strategy, 5 (2018) 52–61.
[37] T. Elango, K.K. Murugavel, The effect of the water depth on the productivity for single and double basin double slope glass solar stills, Desalination, 359 (2015) 82–91.
[38] T. Rajaseenivasan, A.P. Tinnokesh, G. Rajesh Kumar, K. Srithar, Glass basin solar still with integrated preheated water supply – theoretical and experimental investigation, Desalination, 398 (2016) 214–221.
[39] B. Nasri, A. Benatiallah, S. Kalloum, D. Benatiallah, Improvement of glass solar still performance using locally available materials in the southern region of Algeria, Groundwater Sustainable Dev., 9 (2019) 100213, doi: 10.1016/j.gsd.2019.100213.
[40] M. Abu-Arabi, M. Al-harahsheh, M. Ahmad, H. Mousa, Theoretical modeling of a glass-cooled solar still incorporating PCM and coupled to flat plate solar collector, J. Energy Storage, 29 (2020) 101372, doi: 10.1016/j.est.2020.101372.
[41] A. Alaudeen, A.S.A. Thahir, K. Vasanth, A.M.I. Tom, K. Srithar, Experimental and theoretical analysis of solar still with glass basin, Desal. Water Treat., 54 (2015) 1489–1498.
[42] T. Arunkumar, K. Vinothkumar, A. Ahsan, R. Jayaprakash, S. Kumar, Experimental study on various solar still designs, ISRN Renewable Energy, 2012 (2012) 569381, doi: 10.5402/2012/569381.
[43] A. El-Bahi, D. Inan, Analysis of a parallel double glass solar still with separate condenser, Renewable Energy, 17 (1999) 509–521.
[44] B. Nasri, A. Benatiallah, S. Kalloum, D. Benatiallah, Improvement of glass solar still performance using locally available materials in the southern region of Algeria, Groundwater Sustainable Dev., 9 (2019) 100213, doi: 10.1016/j.gsd.2019.100213.
[45] A.M. Manokar, D.P. Winston, Comparative study of finned acrylic solar still and galvanised iron solar still, Mater. Today: Proc., 4 (2017) 8323–8327.

[46] A.M. Manokar, D.P. Winston, Experimental analysis of single basin single slope finned acrylic solar still, Mater. Today: Proc., 4 (2017) 7234–7239.
[47] A.M. Manokar, Y. Taamneh, A.E. Kabeel, D.P. Winston, P. Vijayabalan, D. Balaji, R. Sathyamurthy, S.P. Sundar, D. Mageshbabu, Effect of water depth and insulation on the productivity of an acrylic pyramid solar still – an experimental study, Groundwater Sustainable Dev., 10 (2020) 100319, doi: 10.1016/j.gsd.2019.100319.
[48] A.N. Shmroukh, S. Ookawara, Evaluation of transparent acrylic stepped solar still equipped with internal and external reflectors and copper fins, Therm. Sci. Eng. Prog., 18 (2020) 100518, doi: 10.1016/j.tsep.2020.100518.
[49] P. Pal, R. Dev, Performance study of modified basin-type single-slope solar distiller, Euro-Mediterr. J. Environ. Integr., 3 (2018) 37, doi: 10.1007/s41207-018-0081-x.
[50] M.S.S. Abujazar, S. Fatihah, A.E. Kabeel, Seawater desalination using inclined stepped solar still with copper trays in a wet tropical climate, Desalination, 423 (2017) 141–148.
[51] M.S.S. Abujazar, S. Fatihah, E.R. Lotfy, A.E. Kabeel, S. Sharil, Performance evaluation of inclined copper-stepped solar still in a wet tropical climate, Desalination, 425 (2018) 94–103.
[52] M. Elashmawy, M.M.Z. Ahmed, Enhancing tubular solar still productivity using composite aluminum/copper/sand sensible energy storage tubes, Sol. Energy Mater. Sol. Cells, 221 (2021) 110882, doi: 10.1016/j.solmat.2020.110882.
[53] A.E. Kabeel, M. Abdelgaied, K. Harby, A. Eisa, Augmentation of diurnal and nocturnal distillate of modified tubular solar still having copper tubes filled with PCM in the basin, J. Energy Storage, 32 (2020) 101992, doi: 10.1016/j.est.2020.101992.
[54] H.N. Panchal, P.K. Shah, Improvement of solar still productivity by energy absorbing plates, J. Renewable Energy Environ., 1 (2014) 1–7.
[55] M.K. Gnanadason, P.S. Kumar, V.H. Wilson, A. Kumaravel, Productivity enhancement of a-single basin solar still, Desal. Water Treat., 55 (2015) 1998–2008.
[56] A.K. Thakur, V.P. Chandramohan, Productivity Enhancement of Passive Type Solar Still Using Copper and Aluminum Based Absorber Plate with Al_2O_3 NanoFluid in Water Basin, S. Singh, V. Ramadesigan, Eds., Advances in Energy Research, Vol. 2, Springer Proceedings in Energy, Springer, Singapore, 2020, pp. 273–281.
[57] D.A. Balladin, O. Headley, A. Roach, Evaluation of a concrete cascade solar still, Renewable Energy, 17 (1999) 191–206.
[58] F. Muñoz, E. Barrera, A. Ruiz, E.M. Martínez, N. Chargoy, Long-term experimental theoretical study on several single-basin solar stills, Desalination, 476 (2020) 114241, doi: 10.1016/j.desal.2019.114241.
[59] L.D. Jathar, S. Ganesan, Statistical analysis of brick, sand and concrete pieces on the performance of concave type stepped solar still, Int. J. Ambient Energy, (2020) 1–17, doi: 10.1080/01430750.2020.1848918.
[60] A.M. Manokar, D.P. Winston, A.E. Kabeel, R. Sathyamurthy, Sustainable fresh water and power production by integrating PV panel in inclined solar still, J. Cleaner Prod., 172 (2018) 2711–2719.
[61] A.M. Manokar, M. Vimala, D.P. Winston, R. Sathyamurthy, A.E. Kabeel, Effect of Insulation on Energy and Exergy Effectiveness of a Solar Photovoltaic Panel Incorporated Inclined Solar Still—An Experimental Investigation, A. Kumar, O. Prakash, Eds., Solar Desalination Technology. Green Energy and Technology, Springer, Singapore, 2019, pp. 275–292.
[62] C. Sasikumar, A.M. Manokar, M. Vimala, D.P. Winston, A.E. Kabeel, R. Sathyamurthy, A.J. Chamkha, Experimental studies on passive inclined solar panel absorber solar still, J. Therm. Anal. Calorim., 139 (2020) 3649–3660.
[63] A.M. Manokar, A.E. Kabeel, R. Sathyamurthy, D. Mageshbabu, B. Madhu, P. Anand, P. Balakrishnan, Effect of mass flow rate on fresh water improvement from inclined PV panel basin solar still, Mater. Today: Proc., 32 (2020) 374–378.
[64] A.M. Manokar, D.P. Winston, J.D. Mondol, R. Sathyamurthy, A.E. Kabeel, H. Panchal, Comparative study of an inclined solar panel basin solar still in passive and active mode, Sol. Energy, 169 (2018) 206–216.
[65] A.M. Manokar, M. Vimala, R. Sathyamurthy, A.E. Kabeel, D.P. Winston, A.J. Chamkha, Enhancement of potable water production from an inclined photovoltaic panel absorber solar still by integrating with flat-plate collector, Environ. Dev. Sustainability, 22 (2020) 4145–4167.
[66] A.M. Manokar, Experimental study on effect of different mass flow rate in an inclined solar panel absorber solar still integrated with spiral tube water heater, Desal. Water Treat., 176 (2020) 285–291.
[67] Y. Taamneh, A.M. Manokar, M.M. Thalib, A.E. Kabeel, R. Sathyamurthy, A.J. Chamkha, Extraction of drinking water from modified inclined solar still incorporated with spiral tube solar water heater, J. Water Process Eng., 38 (2020) 101613, doi: 10.1016/j.jwpe.2020.101613.
[68] http://www.primap.com/wsen/Maps/Map Collection/National Maps/Algeria-Satellite-4000x3816.html
[69] A.A. El-Sebaii, M. El-Naggar, Year round performance and cost analysis of a finned single basin solar still, Appl. Therm. Eng., 110 (2017) 787–794.
[70] G.N. Tiwari, S.A. Lawrence, New heat and mass transfer relations for a solar still, Energy Convers. Manage., 31 (1991) 201–203.
[71] G.N. Tiwari, V. Dimri, A. Chel, Parametric study of an active and passive solar distillation system: energy and exergy analysis, Desalination, 242 (2009) 1–18.

Appendix

The evaporative heat transfer coefficient from salty water ($T_{s.w}$), to collector cover ($T_{c.c}$) is calculated by [70,71]:

$$h_{e,w-g} = 16.273 \times 10^{-3} \times h_{c,w-g} \left[\frac{P_w - P_{gi}}{T_{b.w} - T_{gi}} \right] \quad (A1)$$

Convective heat transfer coefficient from $T_{s.w}$, to $T_{c.c}$ is calculated by [70,71]:

$$h_{c,w-g} = 0.884 \left[\left(T_w - T_g\right) + \frac{\left(T_w + 273.15\right)\left(p_w - p_g\right)}{\left(268,900 - p_w\right)} \right]^{1/3} \quad (A2)$$

Partial vapour pressure at the $T_{s.w}$ is calculated by [70,71]:

$$P_w = \exp\left(25.317 - \left(\frac{5,144}{273 + T_{b.w}}\right)\right) \quad (A3)$$

Partial vapour pressure at the $T_{c.c}$ is calculated by [70,71]:

$$P_{gi} = \exp\left(25.317 - \left(\frac{5,144}{273 + T_{gi}}\right)\right) \quad (A4)$$

The thermal efficiency of the single-slope solar still with a steel plate (SSS-SP), SSS with a zinc plate (SSS-ZP) and SSS with a copper plate (SSS-CP) is estimated as [70,71]:

$$\eta_{passive} = \frac{\sum \dot{m}_{ew} L}{\sum I(t) A_s \times 3,600} \times 100 \quad (A5)$$

The exergy efficiency of the SSS-SP, SSS-ZP and SSS-CP is given by [70,71]:

$$\eta_{\text{overall,exe}} = \frac{\sum \text{Ex}_{\text{output}}}{\sum \text{Ex}_{\text{input}}} \tag{A6}$$

The hourly exergy output of the SSS-SP, SSS-ZP and SSS-CP is calculated by [70,71]:

$$\text{Ex}_{\text{output}} = \frac{m_{\text{ew}} L_{\text{fg}}}{3,600} \left[1 - \frac{T_a}{T_w} \right] \tag{A7}$$

The hourly exergy input of the SSS-SP, SSS-ZP and SSS-CP is calculated by [70,71]:

$$\text{Ex}_{\text{input}} = A_w I'(t) \left[1 - \frac{4}{3} \left(\frac{T_a}{T_s} \right) + \frac{1}{3} \left(\frac{T_a}{T_s} \right)^4 \right] \tag{A8}$$